BJRS

BRAZILIAN JOURNAL
OF
RADIATION SCIENCES
09-03 (2021) 01-19

Influence of image reconstruction protocols on the image quality of a small animal PET scanner using ^{18}F and ^{11}C

Barbosa[a,b], J.V C., Gontijo[b], R.M.G., Souza[a,b], G.C.A., Mendes[a], B.M., Silva[a], J.B., Mamede[b], M., Ferreira[a], A.V.

[a] *Nuclear Technology Development Center CDTN/CNEN*
31270-901 Belo Horizonte, MG, Brasil

[b] *Department of Anatomy and Imaging, Federal University of Minas Gerais*
31270-901 Belo Horizonte, MG, Brasil
joaovitorcarmob@gmail.com

ABSTRACT

The small animal positron emission tomography (PET) scanner from Molecular Imaging Laboratory (LIM/CDTN) is dedicated to pre-clinical studies on new ^{18}F and ^{11}C-based radiopharmaceuticals and to the development of novel applications for traditional radiopharmaceuticals. Quality control tests recommended by the NEMA publication NU 4-2008 are routinely carried out to ensure the proper performance of the PET scanner. The aim of this work was to evaluate the influence of image reconstruction protocols on the image quality, accuracy of attenuation and scatter correction parameters for ^{18}F and ^{11}C PET images. ^{18}F-FDG and ^{11}C-PK1122 PET images of the image quality phantom were acquired and then reconstructed using different reconstruction protocols varying algorithms (FBP, MLEM-3D, OSEM-3D), resolution mode (high/standard) and number of iterations (10 to 150). Uniformity, spill-over ratio (SOR) and recovery coefficient (RC) tests were performed for each reconstructed image according to NEMA NU 4-2008. FBP based protocol generated noisier images compared to iterative algorithms (MLEM-3D or OSEM-3D) based protocols. The increase in the number of iterations resulted in higher standard deviation of the analyzed parameters for all images. MLEM-3D and OSEM-3D based protocols generates similar results when the number of iterations and resolution mode were identical. SOR and RC mean values remained stable when the number of iterations ranged from 40 to 150. This study allowed the evaluation of different image reconstruction protocols on important parameters of ^{18}F and ^{11}C PET image quality. Additionally, standard protocols to be adopted in LIM/CDTN for ^{18}F and ^{11}C images reconstruction in preclinical studies were defined.

Keywords: **Small Animal PET, Image Quality, NEMA NU 4-2008.**

ISSN: 2319-0612
Accepted: 2021-09-20

1. INTRODUCTION

Positron emission tomography (PET) is widely used in preclinical trials, generating molecular images applied to biochemical, metabolic and functional investigation of animal organs and tissues. Small animal PET scanners are used in the development of new radiopharmaceuticals or in studies of new applications of traditional radiopharmaceuticals [1]. The small animal PET scanner from Molecular Imaging Laboratory (LIM/CDTN) is dedicated to pre-clinical studies using ^{18}F and ^{11}C-based radiopharmaceuticals.

The quality of the PET molecular image can be affected in different stages of the laboratorial practice, including the step of images acquisition due to intrinsic factors of the PET scanner, or even during the image reconstruction process in which the image reconstruction protocol is executed. The reconstruction algorithm and respective parameters are adjustable on image reconstruction protocol and can be chosen according to each case study (isotope used, size of target structure, etc.).

In order to ensure the better performance of the small animal PET scanner and the optimized image quality, quality control tests must be performed periodically. In 2008, the National Electrical Manufactures Association (NEMA) published its NU 4/2008 standards [2], a consistent and standardized methodology for measuring scanner performance parameters for small animal PET imaging. The publication covers the parameters spatial resolution, scatter fraction, count losses and random coincidence measurements, sensitivity, image quality, accuracy of attenuation and scatter corrections. Thus, results of standardized measurements make possible to compare performances of different small animal PET scanners and can be used for acceptance tests of equipment [2]. To perform these tests, two specific phantoms (devices designed to evaluate image characteristics) and a radioactive point source were necessary.

The goal of this work was to evaluate the influence of the PET image reconstruction protocol on the results of the image quality, accuracy of attenuation and scatter corrections tests preconized by NU 4/2008 standard. The evaluation included ^{18}F and ^{11}C-PET images. Forty-nine different protocols varying the reconstruction algorithms (FBP, MLEM-3D and OSEM-3D), the resolution mode (high/standard) and the number of iterations (10 to 150) were tested for each radionuclide.

2. MATERIALS AND METHODS

Small animal PET scanner:

A small animal PET scanner belonging to the Triumph^{TM} platform, which is dedicated for rodents imaging, was used in this study. The subsystem LabPET 4 consists of a stationary gantry with 1536 detection channels. It uses an Avalanche Photo Diode (APD) detector ring incorporating an assembly of Lutetium Yttrium oxyorthosilicate – $Lu_{1.9}Y_{0.1}SiO_5$ (LYSO) and Lutetium Gadolinium oxyorthosilicate – $Lu_{0.4}Gd_{1.6}SiO_5$ (LGSO) scintillators optically coupled [3]. LabPET 4 images are acquired using a 250-650 keV energy window and 22 ns coincidence timing window. It provides axial field of view (FOV) of 3.7 cm and can operate in dynamic or static mode. Coincident data are saved in list mode and can be displayed as sinograms. More details about the LabPET 4 design and architecture are presented elsewhere [4, 5]. The system is equipped with LabPET 1.12.1 software supplied by the PET scanner manufacturer [6].

NEMA NU 4-2008 tests:

It is important to remark that in Brazil there is no national regulatory requirement for quality control or performance testing for small animal PET scanners [7]. Therefore, this work was based on some tests preconized by NEMA NU 4/2008. Additionally, most of Brazilian preclinical molecular imaging services do not have a quality assurance program in place for their imaging systems [7].

For imaging capabilities evaluation the NEMA NU 4/2008 recommends using a specific Image Quality (IQ) phantom (Figure 1). IQ phantom is made up of polymethylmethacrylate (PMMA) with internal dimensions of 50 mm length and 30 mm diameter. It presents a main chamber that communicates with five different diameters auxiliary rods (1, 2, 3, 4, and 5mm), all of which are expected to be filled with a radiopharmaceutical water solution. In addition, the IQ phantom presents two *cold* chambers - to be filled with air and water, both non-radioactive. Details of IQ phantom are presented at NEMA NU 4-2008 [2]. The different regions of the IQ phantom (main chamber, auxiliary rods and cold chambers) are used to evaluate different parameters of imaging capabilities of scanner, discussed further below.

For ^{18}F studies, PET image acquisition procedure followed NEMA NU 4-2008 (3.7 MBq at the beginning of acquisition, 20 min acquisition time) recommendation. For ^{11}C studies, NEMA NU 4-2008 recommendations were adapted (3.7 MBq at the beginning of acquisition, 30 min acquisition time) to assure the same number of positron emissions during the image acquisition, considering half-life and branching ratio of each radionuclide. The activity in the phantom was measured in a Capintec CRC®-25R activity meter. An implemented Quality Assurance Program [8], based on the national standards [9] and the manufacturer's manual [10], assures the activity meter performance.

The IQ phantom filled with radiopharmaceutical (^{18}F-FDG or ^{11}C-PK1112) solution was placed in the center of the axial FOV (Figure 1C) and measured with the LIM/CDTN typical whole-body imaging protocol which uses three bed positions in order to cover the phantom length. Decay corrections were automatically done by LabPET 1.12.1 software, in order to adjust the acquisition time for each bed position. Both radiopharmaceuticals were provided by the Radiopharmaceutical Research and Production Unit (UPPR/CDTN).

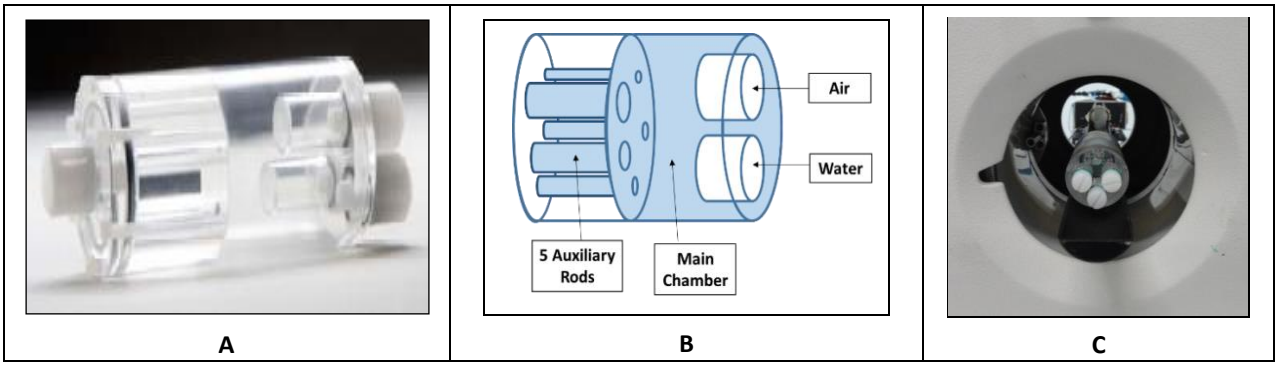

Figure 1: *Image Quality phantom. A: Photo gallery of authors; B: schematic representation where blue indicates radiopharmaceutical fillable volumes; C: phantom positioned on PET scanner FOV.*

Protocols for Images Reconstruction:

In order to determine the influence of the PET image reconstruction protocols on image quality, accuracy of attenuation and scatter corrections tests preconized by NU 4-2008 standards, forty nine different image reconstruction protocols (Table 1) were studied, varying reconstruction algorithm, number of iterations and resolution mode - (0.50 x 0.50 x 0.50) mm^3 voxel size in standard resolution mode or (0.25 x 0.25 x 0.50) mm^3 voxel size in high resolution mode.

Table 1: PET image reconstruction protocols applied to the ^{18}F and ^{11}C images of the IQ Phantom.

Reconstruction Algorithm	Resolution	Number of Iterations
FBP	--	--
MLEM-3D	Standard	10i; 20i ... 100i; 120i; 150i
	High	
OSEM-3D (4 sub-sets)	Standard	
	High	

PET Images Analysis:

After image reconstructions, scanner performance tests recommended by the NEMA 4-2008 (section 6) were carried out, namely: Uniformity, Spill-Over Ratio (SOR) and Recovery Coefficient (RC).

The Uniformity test consists of obtaining mean, maximum, minimum and standard deviation of the activity concentration in the main chamber. To perform the test, a central cylindrical volume of interest (VOI) with 22.5 mm diameter and 10 mm height was analyzed. The number of counts per second (cps) in the VOI were converted in activity concentration (kBq.ml^{-1}) using a previous calculated conversion coefficient. This coefficient was obtained by measuring a 10 ml cylindrical phantom filled with known activity (3MBq; ^{18}F-FDG or ^{11}C-PK1112) to determine the relationship between kBq and cps in a VOI. The activity concentration percentage standard deviation (%SD) or image roughness (%IR) [11], was evaluated according to equation 1:

$$\%SD = \%IR = 100 \times \frac{AC_{SD}}{AC_{mean}} \qquad (1)$$

where: AC_{mean} is the mean activity concentration measured in the VOI positioned in the IQ phantom main chamber and AC_{SD} is the respective standard deviation. The uniformity in the main chamber is an indicative of attenuation and scatter correction performance of the PET scanner [2].

The ratio between the mean activity measured in a *cold* chamber (filled with air or water) and the mean activity measured in the main chamber provides the Spill-Over Ratio. To perform this test, a central cylindrical VOI (4 mm diameter, 7.5 mm height) in each cold chamber was analyzed. SOR test results are an indicative of scatter correction performance of the PET scanner [2].

The ratios between the mean activity measured in each one of the five auxiliary rods and the mean activity measured in the main chamber provides the image Recovery Coefficients. The RCs are indicative of the spatial resolution of the PET scanner [2]. To perform this test, the 10 mm length central region of each rod was average to obtain a single image in which the coordinates of the highest value pixel were determined. Then, for each rod, the mean activity concentration was determined considering a 10 mm axial line passing through the highest value pixel ($MEAN_{\text{line profile}}$). RC value and RC standard deviation were determined according equation 2 and 3 respectively [2], where BG refers to background.

$$RC = \frac{(MEAN_{\ line\ profile} - MEAN_{\ BG})}{MEAN_{\ Uniformity}} \quad (2)$$

$$\%SD_{RC} = 100 \times \sqrt{\left(\frac{SD_{\ line\ profile}}{MEAN_{\ line\ profile}}\right)^2 + \left(\frac{SD_{\ BG}}{MEAN_{BG}}\right)^2} \quad (3)$$

More details of analysis for image quality tests are provided in NEMA 4-2008 and also in a previous work [12]. Image quantitative analyses were performed using PMOD® software, v3.7 [13].

3. **RESULTS AND DISCUSSION**

Figure 2 and 3 presents ^{18}F and ^{11}C PET images obtained using different image reconstruction protocols. A qualitative analysis of the Figures revels that ^{11}C PET images are rougher than ^{18}F images. For each radionuclide, FPB algorithm based protocol generated rougher images when compared to MLEM-3D or OSEM-3D algorithm based protocols. Additionally, it is possible to see that MLEM-3D and OSEM-3D based protocols generated similar images when same reconstruction parameters (number of iterations and resolution mode) were used. By increasing the number of iterations the image roughness was reduced to a certain point after which the roughness started to increase again. These observations will be discussed further below where the results of quantitative analysis are presented.

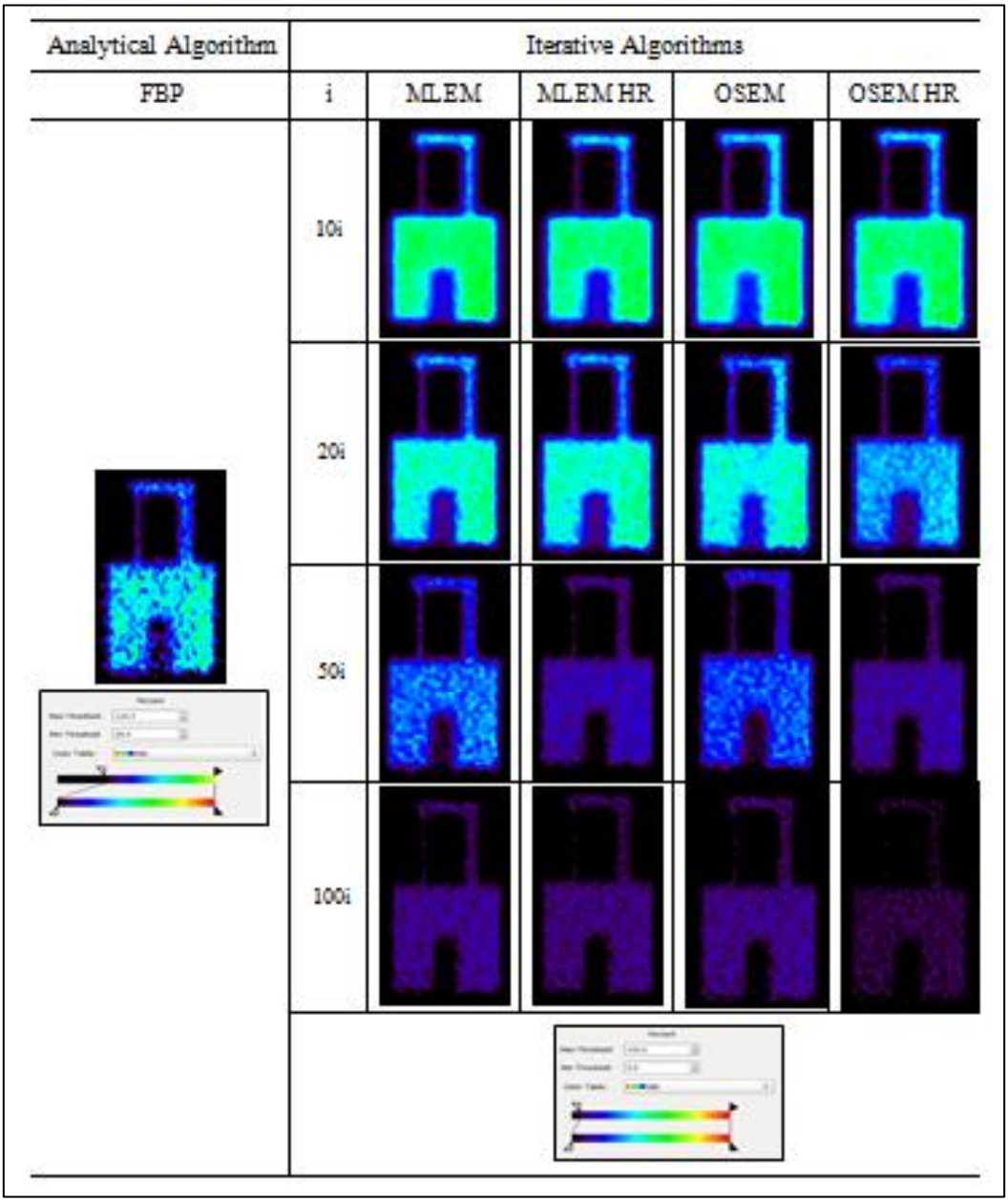

Figure 2: *^{18}F-FDG PET images of the IQ phantom. Reconstruction protocols varied algorithm (FBP, MLEM-3D, OSEM-3D), resolution mode (standard/high), number of iterations.*

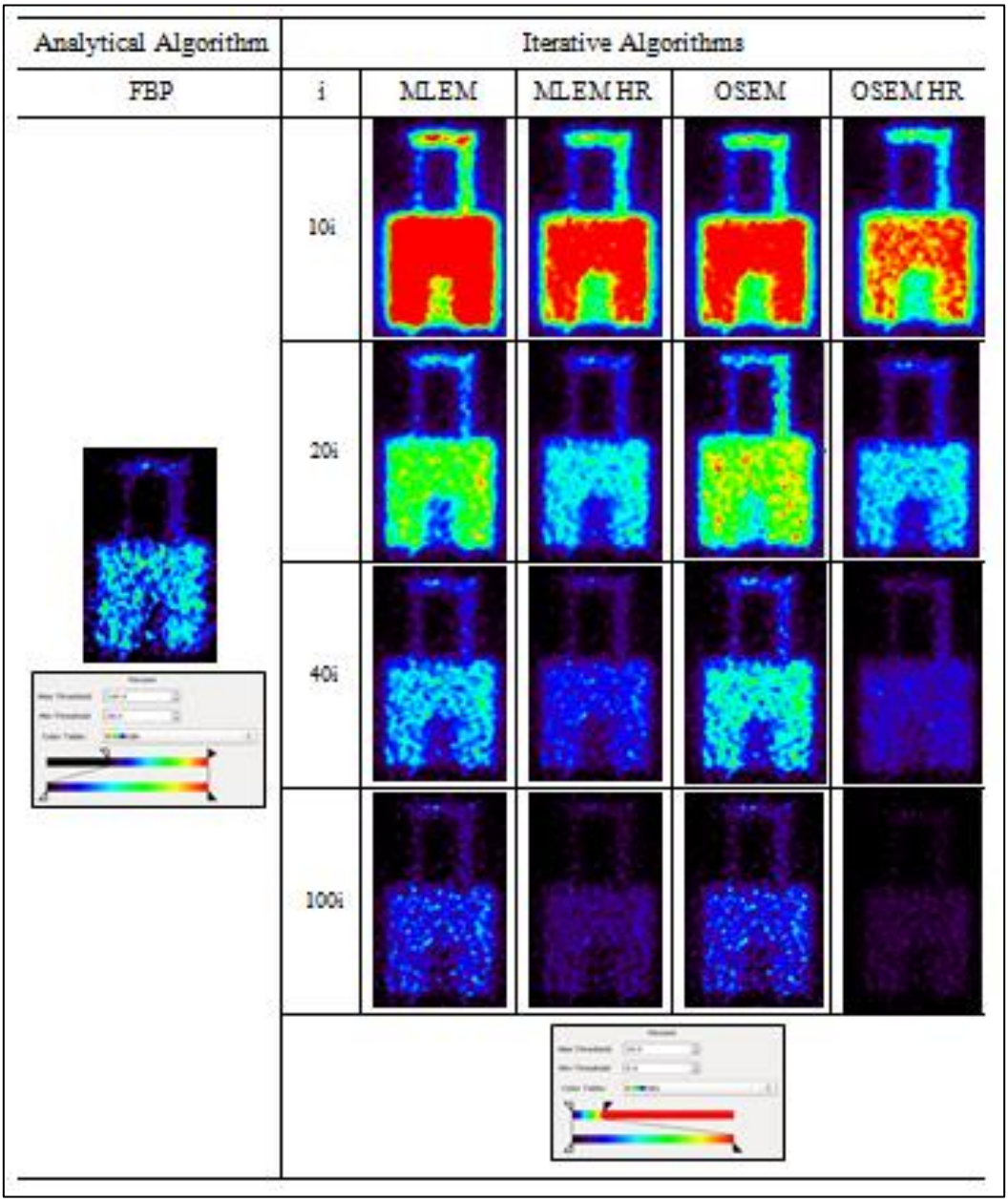

Figure 3: *^{11}C-PK112 PET images of the IQ phantom. Reconstruction protocols varied algorithm (FBP, MLEM-3D, OSEM-3D), resolution mode (standard/high), number of iterations).*

3.1. Uniformity Test

Table 2 shows the results of the uniformity test for ^{18}F and ^{11}C PET images reconstructed using the analytical FBP algorithm based protocol. The mean value of activity concentration in both

studies was higher than the injected activity into the IQ phantom (168 MBq·mL^{-1}). This fact, observed also in a previous work [12], is explained by the use of a second phantom to determine the conversion coefficient (cps·mL^{-1} to kBq·mL^{-1}). As this second phantom has a smaller volume than the IQ phantom, less attenuation is expected, which results in a higher counting efficiency.

Table 2: Uniformity test results for PET images reconstructed using FBP based protocol.

Isotope	Mean Activity Concentration (kBq · mL $^{-1}$)	SD (%)
^{18}F	195	18
^{11}C	185	40

As seen in the qualitative analysis of the FBP reconstructed PET images, ^{11}C image presented a higher roughness when compared to the ^{18}F image: ^{11}C image roughness (40%) was more than twice the value obtained for the ^{18}F image (18%). This found is explained by differences in nuclear properties of the radionuclides. ^{11}C mean positron range in water (1.2 mm) is greater than the ^{18}F one (0.6 mm) [14]. Positron range generates an error in the localization of the true position of the positron emission since coincidence detection is related to the location of positron annihilation.

Results of the uniformity test for PET images reconstructed using protocols based in MLEM-3D and OSEM-3D iterative algorithms are presented in Figure 4. For all protocols, concentration activity results were greater than the injected activity as discussed before. In general, results showed stable values of the activity concentration mean, around 192 kBq·mL^{-1} for ^{18}F PET images and 180 kBq·mL^{-1} for ^{11}C PET images, regardless of the reconstruction protocol. However, a significant increase in the activity concentration standard deviation was observed as the number of iterations increased for both radionuclides and both reconstruction algorithm, regardless the resolution mode used. Considering MLEM-3D based protocols using standard resolution, the activity concentration for ^{18}F PET image were 192 kBq · mL^{-1} ± 4% using 10 iterations and 192 kBq·mL^{-1} ± 27% using 150 iterations. In a similar way, considering MLEM-3D reconstructions of ^{11}C PET image using standard resolution, the values of activity concentration were 180 kBq·mL^{-1} ± 8% using MLEM with 10 iterations, and 180 kBq·mL^{-1} ± 59% using MLEM with 150 iterations. In both cited examples, the standard deviation of activity concentration increased approximately seven times

when the number of iterations ranged from 10 to 150. Depending on the number of iterations, the image roughness was higher than the obtained for FBP algorithm. This behavior is well known and Defrise et al. (2006) have mentioned that there should be a compromise between the Poisson likelihood and image roughness [15].

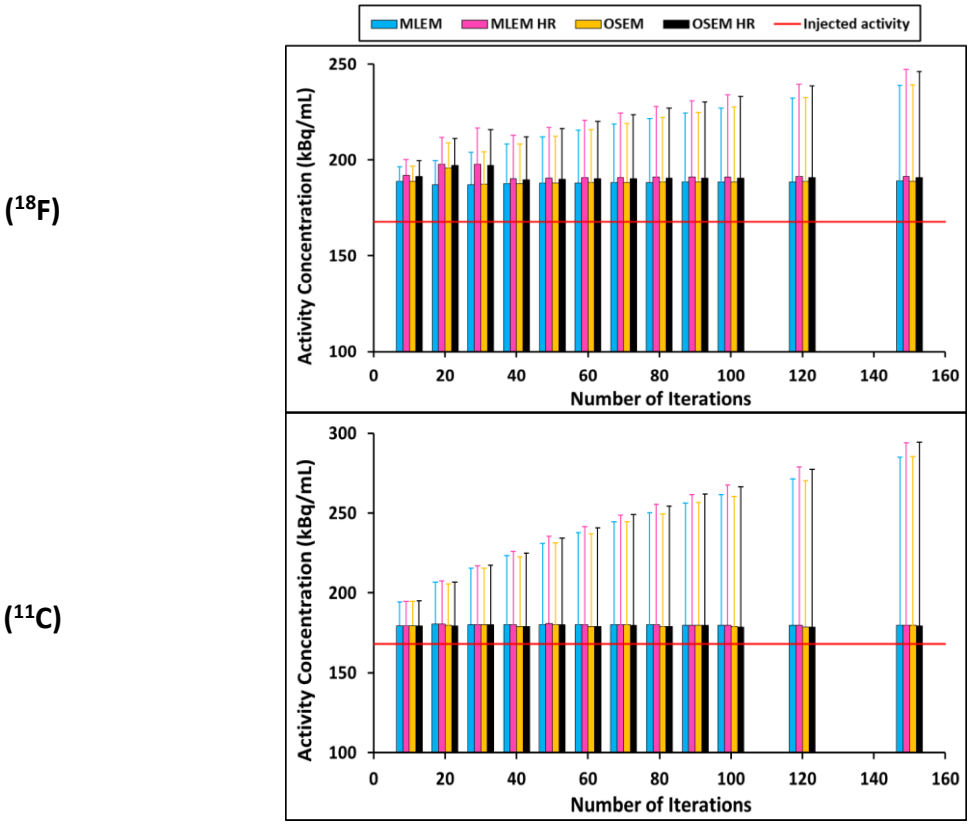

Figure 4: *IQ phantom main chamber activity concentration mean and respective standard deviation for ^{18}F and ^{11}C PET images reconstructed with MLEM-3D and OSEM-3D based protocols. (HR: high resolution).*

3.2. Spill-over Ratio

Table 3 shows the results of the spill-over ratio test obtained for ^{18}F and ^{11}C PET images reconstructed using the analytical FBP algorithm based protocol. All the SOR values presented a large standard deviation (SD), typical for using FBP reconstruction algorithm. The main source of this large SD is the variance in the data originated from the *cold* chambers filled with air or water.

Table 3: Spill-over Ratio test results for FBP based reconstruction protocol

Radionuclide	SOR_Air	SOR_Water
^{18}F	0.28 ± 61%	0.08 ± 190%
^{11}C	0.23 ± 158%	0.10 ± 357%

Figure 5 shows the results of the spill-over ratio tests for ^{18}F PET images reconstructed using MLEM-3D and OSEM-3D iterative algorithms based protocols.

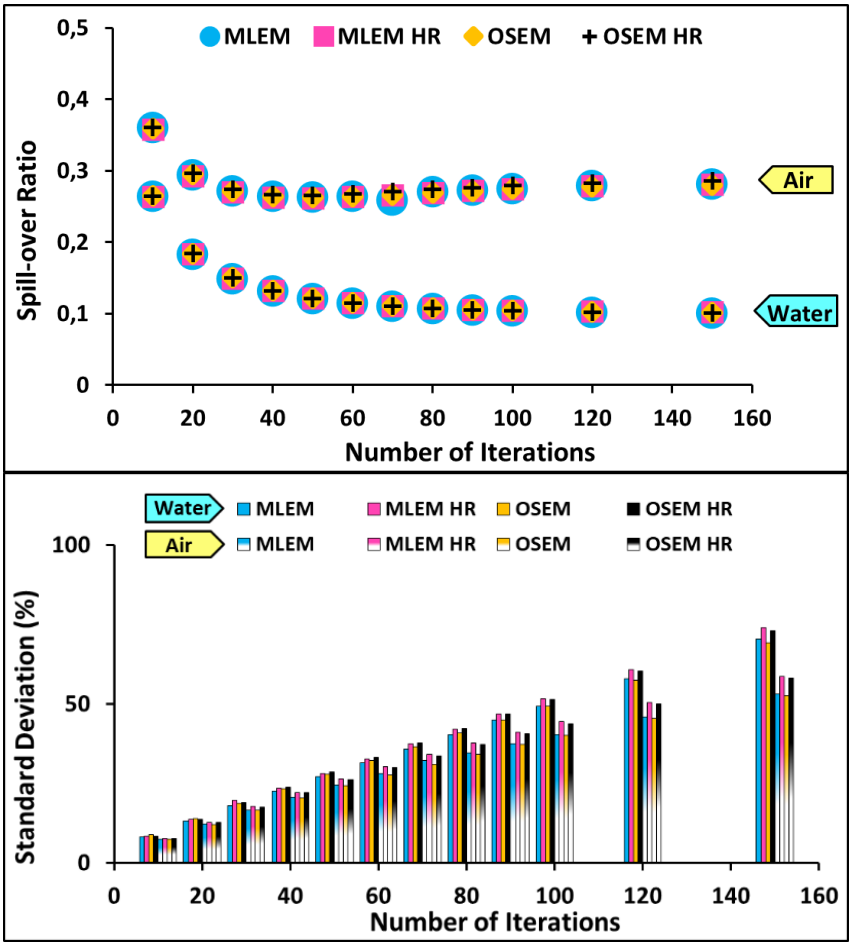

Figure 5: *Spill-over ratios and respective standard deviations for ^{18}F PET images reconstructed with MLEM-3D and OSEM-3D based protocols (HR: High resolution).*

Results in Figure 5 indicates that for air chamber the spill-over ratio value for ^{18}F PET images remained practically stable (SOR ≈ 0.27) after 20 iterations regardless of the reconstruction algorithm, MLEM-3D or OSEM-3D. For the water chamber the SOR value remained stable after 40 iterations (SOR ≈ 0.13). However, the standard deviation associated with the spill-over ratio increased steadily with the increase in the number of iterations for all image reconstruction protocols. For MLEM-3D with 10 iterations, regardless the resolution mode, the spill-over ratio percentage standard deviation was around 7.5% for air and 8.3% for water. For MLEM with 150 iterations, the spill-over ratio percentage standard deviation was 53% for air and 70% for water for protocol using standard resolution, and 59% for air and 74% for water for protocol using high resolution. Due to the small voxel dimensions in high resolution mode, the voxel count should be poorer than in standard resolution mode. This could be the reason for larger SD observed for high resolution reconstructions with iteration numbers higher than 30.

In a general way, the use of MLEM-3D or OSEM-3D based reconstruction protocols for ^{18}F PET image reconstruction led to similar results, when the parameters resolution mode and number of iterations were the same. This found was also expected since OSEM is based in a simple modification of MLEM algorithm, designed to accelerate the convergence (although it is not guaranteed for OSEM) [15].

Figure 6 shows the results of the spill-over ratio tests for ^{11}C PET images reconstructed using the MLEM-3D and OSEM-3D iterative algorithm based protocols. Results indicated that for both *cold* chambers, water and air, the spill-over ratio values obtained for ^{11}C PET images remained practically stable after 40 iterations (0.12 for water and 0.26 for air) for both MLEM-3D and OSEM-3D algorithm based reconstruction protocols. However, as observed for ^{18}F PET images, the standard deviation associated with the spill-over ratio increased steadily with the increase in the number of iterations for both cases. For MLEM-3D with 10 iterations, regardless resolution mode, the percentage standard deviation remained around 16% for both *cold* chambers. For MLEM-3D with 150 iterations, the standard deviation for protocol using standard resolution mode was 149% for air and 144% for water, and for high resolution 154% for air and 150% for water. In a general way, as observed for ^{18}F images, the use of MLEM-3D or OSEM-3D based protocols for ^{11}C PET image reconstruction led to similar results, when the parameters resolution mode and number of iterations were the same.

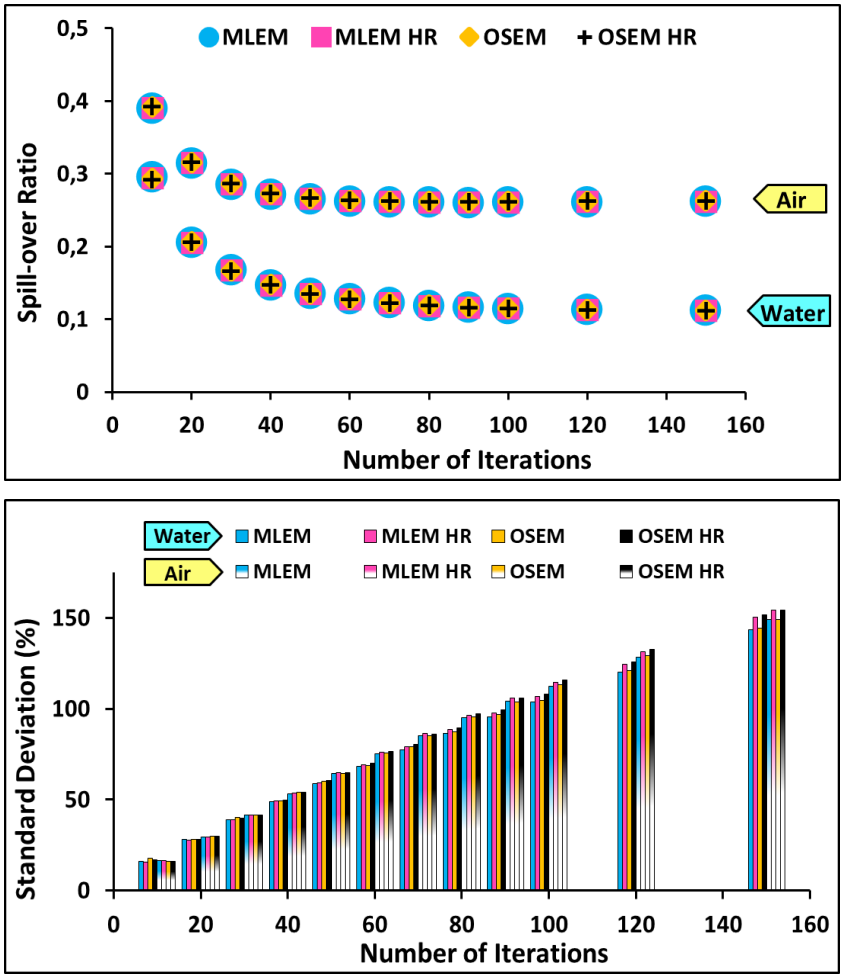

Figure 6: *Spill-over ratios and respective standard deviations for ^{11}C PET images reconstructed with MLEM-3D and OSEM-3D based protocols (HR: High resolution).*

3.3. Recovery Coefficients

Table 4 shows the results of the recovery coefficients test for ^{11}C and ^{18}F PET images reconstructed using the analytical FBP algorithm based protocol. The results show that recovery coefficients were higher for the ^{18}F images when compared to the ^{11}C ones. However, standard deviations in both cases were very high, especially for the ^{18}F case.

Figures 7 and 8 shows the results of the recovery coefficients tests for ^{18}F PET images reconstructed using iterative algorithms based protocols. Similarly, Figures 9 and 10 show the recovery coefficients for ^{11}C PET images reconstructed using iterative algorithms-based protocols.

Table 4: Recovery coefficients obtained with FBP based protocol.

Rod diameter (mm)	Recovery Coefficient	
	^{18}F	^{11}C
1	0,17 ± 349%	0,00 ± 91%
2	0,38 ± 164%	0,22 ± 67%
3	0,58 ± 164%	0,29 ± 60%
4	0,76 ±164%	0,42 ± 61%
5	0,87 ±163%	0,56 ± 55%

Results presented in Figure 7 revealed that, in general, the use of the high-resolution mode for ^{18}F PET image reconstruction did not result in an expressive improvement of the recovery coefficient values. This fact was observed for both studies, using MLEM-3D or OSEM-3D iterative algorithm based protocols. For the protocols using MLEM-3D with 10 iterations, the RC values for the diameters from 1 mm to 5 mm ranged from 0.03 to 0.83 in studies using standard resolution or high resolution mode. For the reconstruction protocol using MLEM-3D with 150 iterations, the RC values for diameters from 1 mm to 5 mm ranged from 0.22 to 0.88, using standard resolution, and from 0.27 to 0.85, using high resolution. Additionally, the use of high resolution mode made the RCs for 4 mm diameter rod larger than those observed for 5 mm; figure 7 shows that the 4 mm curve is superior to the 5 mm curve, indicating "better recovery". Probable, this found is due to the test design: the mean activity concentration is determined considering a 10 mm axial line passing through the highest value pixel in an average image. At high resolution mode smaller voxels are used (a quarter of the standard resolution mode voxel volume), which can cause an increase in the average activity concentration, depending on image roughness.

For OSEM-3D based protocol with 10 iterations, the RC values for diameters from 1 mm to 5 mm ranged from 0.02 to 0.82 in studies using standard or high resolution mode. For the OSEM-3D study with 150 iterations, the RC values for diameters from 1 mm to 5 mm ranged from 0.21 to 0.90, using standard resolution and from 0.28 to 0.83, using high resolution.

As observed previously in other tests, the increase in the number of iterations resulted in larger values of the recovery coefficient standard deviations (Figure 8).

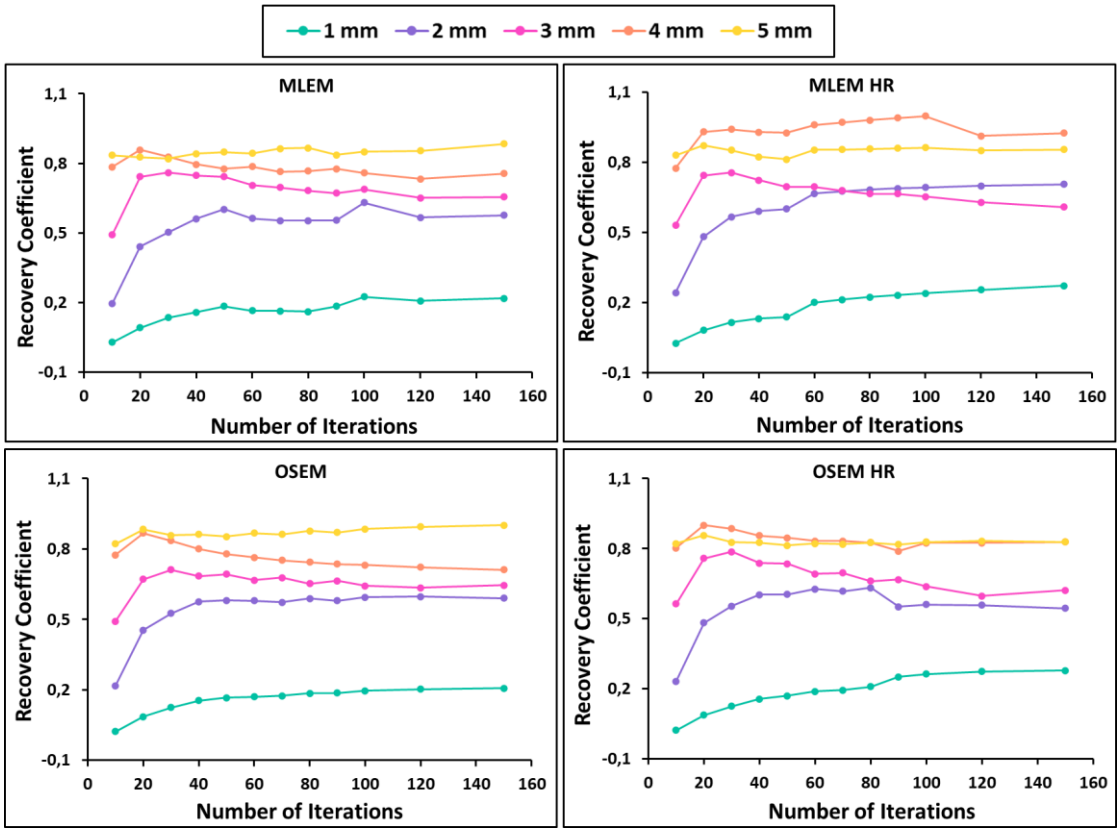

Figure 7: *Recovery coefficients for ^{18}F PET images reconstructed using iterative algorithm based protocols. (HR: High resolution)*

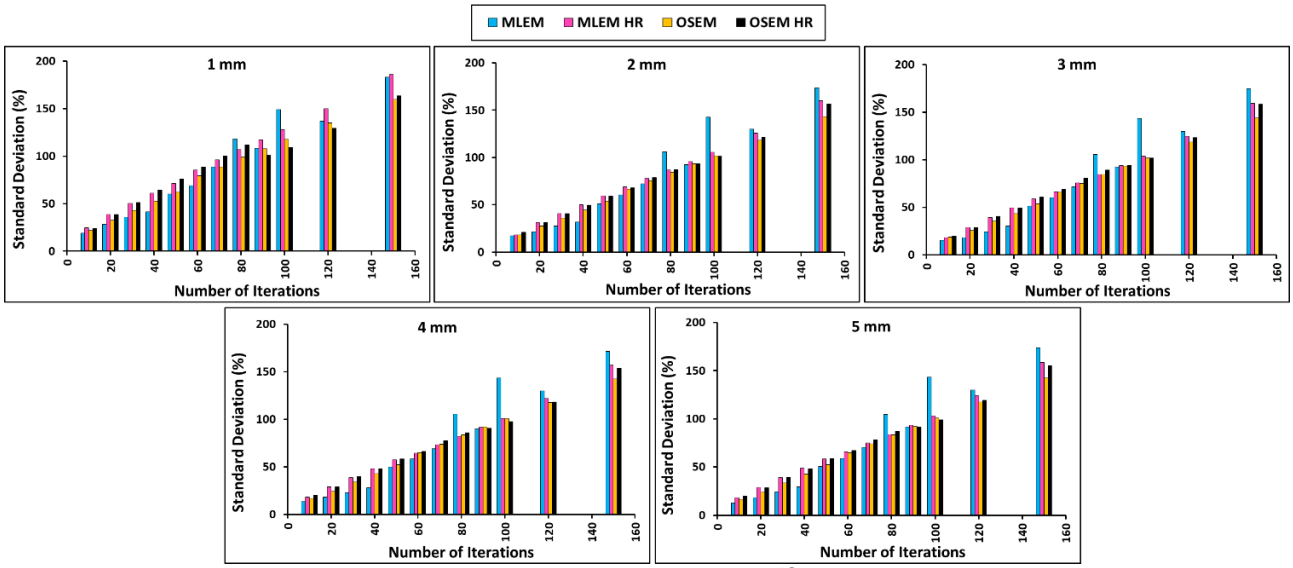

Figure 8: *Recovery coefficients standard deviations for ^{18}F PET images reconstructed using iterative algorithm based protocols. (HR: High resolution)*

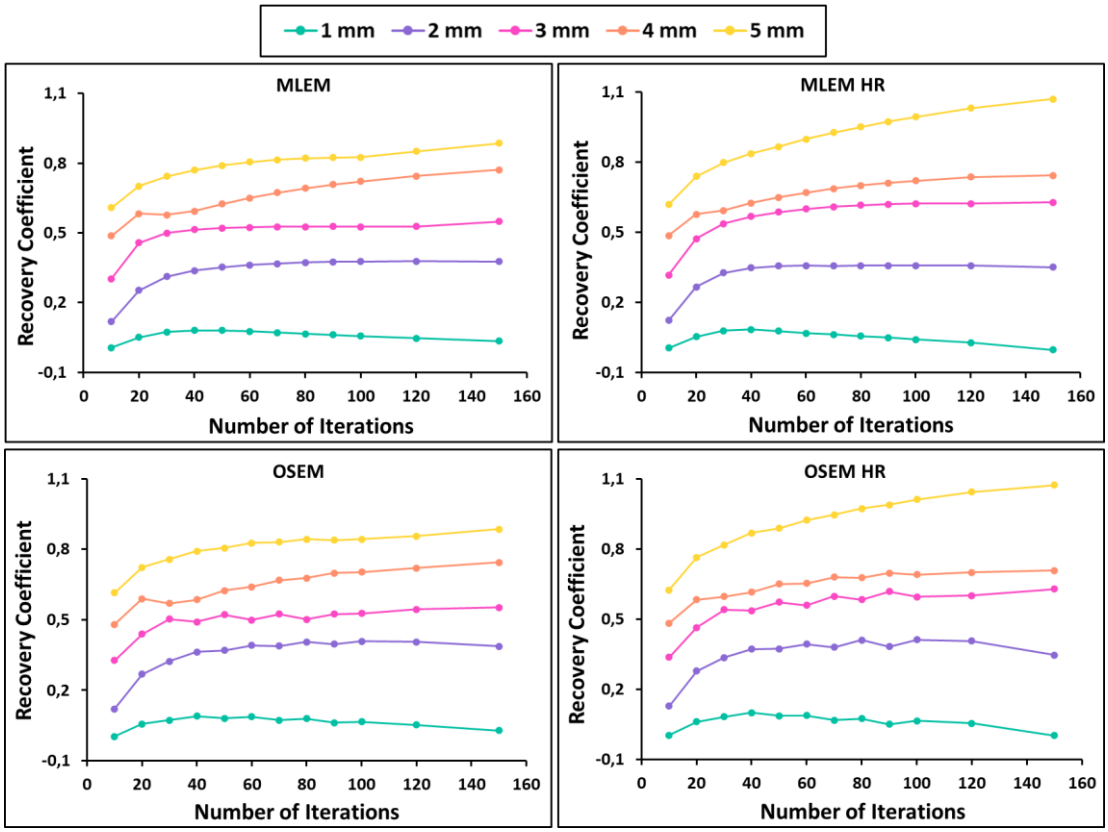

Figure 9: *Recovery coefficients for ^{11}C PET images reconstructed using iterative algorithm based protocols. (HR: High resolution)*

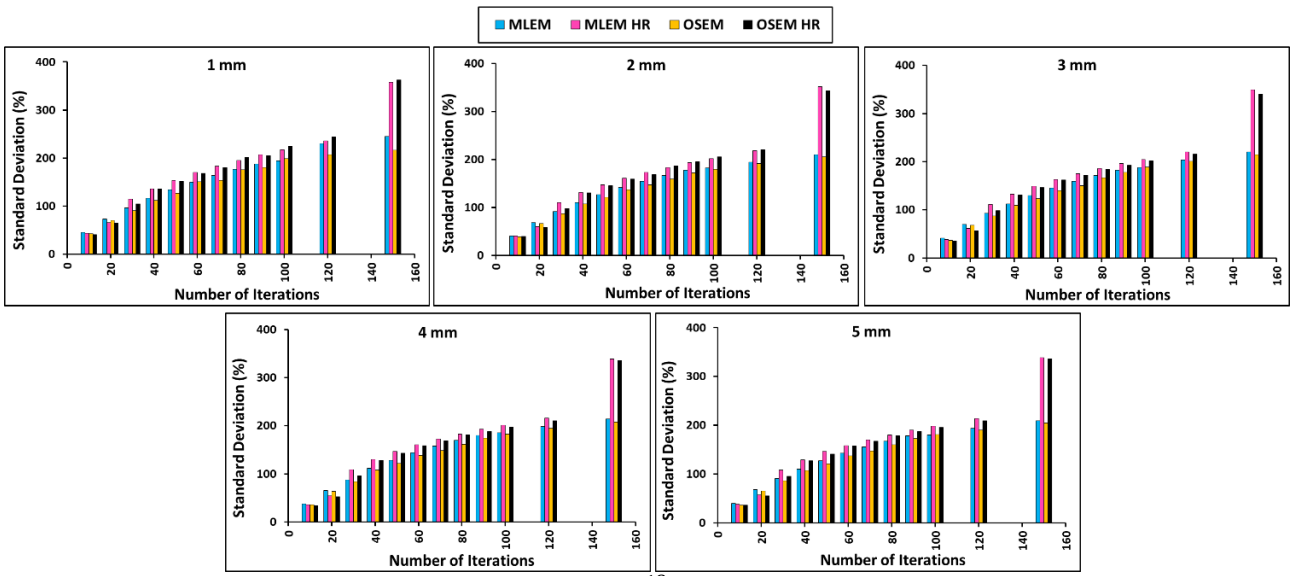

Figure 10: *RCs standard deviations for ^{18}F PET images reconstructed using iterative algorithms. (HR: High resolution)*

Similarly to observed in Figure 7, Figure 9 shows that the use of the high-resolution mode in protocols for ^{11}C PET image reconstruction did not result in an expressive improvement of the recovery coefficient values. This fact was observed for both studies, using MLEM-3D or OSEM-3D iterative algorithm based protocols. For the protocol using MLEM-3D with 10 iterations, the RC values for the diameters from 1 mm to 5 mm ranged from 0.01 to 0.61 using standard resolution, and from 0.01 to 0.62 using high resolution. In a similar way, for the protocol using MLEM-3D with 150 iterations, the RC values for diameters from 1 mm to 5 mm ranged from 0.03 to 0.89 using standard resolution, and from 0.00 to 1.07 using high resolution. For OSEM-3D based protocol with 10 iterations, the RC values for diameters from 1 mm to 5 mm ranged from 0.00 to 0.61 using standard resolution and from 0.00 to 0.62 using high resolution. In a similar way, for the OSEM-3D based protocol with 150 iterations, the RC values for diameters from 1 mm to 5 mm ranged from 0.03 to 0.88 using standard resolution, and 0.00 to 1.07 using high resolution.

As observed in the ^{18}F study, the increase in the number of iterations resulted in larger values of the recovery coefficient standard deviations (Figure 10) of the ^{11}C PET images.

In general, it was observed that iterative algorithms provided a better signal-to-noise ratio (lower roughness of the images) and better visibility of the contours of the phantoms than FBP algorithm, especially for 10 to 40 iterations. All algorithms studied here presented similar results for spill-over ratio and recovery coefficients. MLEM-3D and OSEM-3D algorithms are known to have longer reconstruction times than FBP [15]. However, considering the processing capacity of current computers, it was not considered a limiting factor for the reconstruction of small animal PET images.

The results of this work permitted to know the influence of the PET image reconstruction protocol on the results of the image quality, accuracy of attenuation and scatter corrections tests preconized by NU 4/2008 standards as discussed above.

Additionally, this study permitted to define standard image reconstruction protocols to be adopted in the LIM/CDTN laboratorial routine for ^{18}F and ^{11}C PET images in preclinical studies. For the protocols definition, some aspects were taken into account: (i) the iterative algorithms provided better image quality than FBP analytical algorithm; (ii) number of iterations should not be so low in which the recovered information are insufficient, nor so high for which there are great

associated uncertainties; and (iii) the use of high resolution mode did not improve expressively the tests results.

Table 5 shows the protocols implemented in LIM/CDTN laboratorial routine for ^{18}F and ^{11}C PET preclinical studies.

Table 5: Standard PET images reconstruction protocols adopted in LIM/CDTN

Isotope	Algorithm	Resolution Mode	Number of Iterations
^{18}F	MLEM-3D	Standard	20
^{11}C			40

4. CONCLUSION

This work allowed us to determine the influence of PET image reconstruction protocols on the values of the image quality parameters stablished according NEMA NU4-2008 standards.

The PET image reconstruction protocols based in iterative algorithms (MLEM-3D and OSEM-3D) generated images with lower roughness and better visual quality than FBP in this study. In general, MLEM-3D and OSEM-3D based protocols generates similar results when the number of iterations and resolution mode were identical. In general, the quantitative analysis showed that the iterative based protocols lead to better quality of the PET image evaluated by the parameters uniformity, spill-over ratio and recovery coefficients. Additionally, this study supported the definition of the standard protocols for PET image reconstruction to be adopted in the LIM/CDTN laboratorial routine for processing ^{18}F or ^{11}C images in preclinical studies.

ACKNOWLEDGMENT

Authors thanks CDTN/CNEN, PIBIC/CNPq, FAPEMIG and UFMG for supporting this work.

REFERENCES

[1] R. YAO, R.; LECOMTE, R.; CRAWFORD, E. Small-Animal PET: What is it, and why do we need it? **J Nucl Med Technol**, v. 40-03, p.157-165, 2011.

[2] NEMA - National Electrical Manufacturers Association. **Performance Measurements of Small Animal PET**, Rosslyn VA; Standards Publication NU 4-2008, 2008.

[3] GE Healthcare, **Triumph Service Guide**, Technical Publication, © GE Healthcare, Revision Draft 6, USA (2011).

[4] TRETRAULT M. A., *et al*. System architecture of the LabPET small animal PET scanner. **IEEE Trans Nucl Sci**, v. 55, p. 2546-2550, 2008.

[5] FONTAINE R., *et al*. The hardware and signal processing architecture of LabPET™, a small animal APD-based digital PET scanner **IEEE Trans Nucl Sci**, v. 56, p. 3-9, 2009.

[6] Gamma Medica-Ideas, **Positron Emission Tomography (PET) Scanner Software - Manual for Acquisition and Processing of PET Images from the LABPET System**, 2011.

[7] GONTIJO, R.M.G., *et al*., Quality control of small animal PET scanner: The Brazilian Scenario. **Braz J Rad Sci**, v. 08-02, p. 01-09, 2020.

[8] GONTIJO, R.M.G., *et al*., Constancy tests and quality assurance of the activimeters used in a radiopharmaceutical production facility. **Braz J Rad Sci**, v. 07-2A, p. 01-13, 2019.

[9] CNEN - Comissão Nacional de Energia Nuclear. **Requisitos de segurança e proteção radiológica para serviços de medicina nuclear,** Norma CNEN NN 3.05, 2013.

[10] CAPINTEC, Inc. **Owner´s Manual**. Copyright 2006. Revision H, 2015.

[11] BELCARI, N. *et al*., NEMA NU-4 Performance Evaluation of the IRIS PET/CT Preclinical Scanner. **IEEE Trans Nucl Sci**, v. 1, p. 301-309, 2017.

[12] GONTIJO, R.M.G., *et al*. Image quality evaluation of a small animal PET scanner. **Braz J Rad Sci**, v. 8-01, p. 01-13, 2020.

[13] PMOD Technologies LCC, **PMOD v.3.7 User Manual**. 2015.

[14] IAEA - International Atomic Energy Agency. Live Chart of Nuclides. https://www-nds.iaea.org/relnsd/vcharthtml/VChartHTML.html. 2020.

[15] DEFRISE, Michel & Kinahan, Paul & Michel, Christian. (2006). **Image Reconstruction Algorithms in PET**. 10.1007/1-84628-007-9_4.